(32) S. F. A. Kettle, *Inorg. Chem.*, **4**, 1661 (1965).

(33) For a perceptive analysis of the σ- and π-bonding capabilities of CO, $N_2$, and $CN^-$ see (a) K. G. Caulton, R. L. DeKock, and R. F. Fenske, *J. Am. Chem. Soc.*, **92**, 515 (1970); (b) R. L. DeKock, A. C. Sarapu, and R. F. Fenske, *Inorg. Chem.*, **10**, 38 (1971); (c) A. C. Sarapu and R. F. Fenske, *ibid.*, **14**, 247 (1975).

(34) G. Herzberg, "Spectra of Diatomic Molecules", Van Nostrand, Princeton, N.J., 1950, pp 522, 553.

(35) J. Chatt, D. P. Melville, and R. L. Richards, *J. Chem. Soc. A*, 2841 (1969).

(36) (a) D. Cullen, E. Meyer, Jr., T. S. Srivastava, and M. Tsutsui, *J. Chem. Soc., Chem. Commun.*, 584 (1972); (b) J. J. Bonnet, S. S. Eaton, G. R. Eaton, R. H. Holm, and J. A. Ibers, *J. Am. Chem. Soc.*, **95**, 2141 (1973).

(37) V. L. Goedken and S.-M. Peng, *J. Chem. Soc., Chem. Commun.*, 914 (1974).

(38) (a) E. J. Heidner, R. C. Ladner, and M. F. Perutz, *J. Mol. Biol.*, **104**, 707 (1976); (b) J. C. Norvell, A. C. Nunes, and B. P. Schoenborn, *Science*, **190**, 568 (1975); (c) R. Huber, O. Epp, and H. Formanek, *J. Mol. Biol.*, **52**, 349 (1970).

(39) (a) P. A. Bretscher, Ph.D. Dissertation, University of Cambridge, 1968; (b) W. A. Hendrickson and W. E. Love, *Nature (London), New Biol.*, **232**, 197 (1971); (c) J. F. Deatherage, R. S. Loe, C. M. Anderson, and K. Moffat, *J. Mol. Biol.*, **104**, 687 (1976).

(40) A calculation on the mode of attack of alkyl halides on $Co(CN)_5{}^{3-}$ yields a similar nonlinear reaction path: K. Ohkubo, H. Kanaeda, and T. Tsuchihashi, *Bull. Chem. Soc. Jpn.*, **46**, 3095 (1973).

(41) This excludes bridging $O_2$ as well as those complexes containing more than one $O_2$ per metal center.

(42) An initial report of a linear Co–O–O in $Co(CN)_5O_2{}^{3-}$ [L. D. Brown and

K. N. Raymond, *J. Chem. Soc., Chem. Commun.*, 470 (1974)] was later revised to a 153° bent structure [L. D. Brown and K. N. Raymond, *Inorg. Chem.*, **14**, 2595 (1975)].

(43) J. P. Collman, R. R. Gagne, C. A. Reed, W. T. Robinson, and G. A. Rodley, *Proc. Natl. Acad. Sci. U.S.A.*, **71**, 1326 (1974).

(44) B. M. Hoffman, D. L. Diemente, and F. Basolo, *J. Am. Chem. Soc.*, **92**, 61 (1970).

(45) E.-I. Ochiai, *J. Inorg. Nucl. Chem.*, **35**, 1727, 3389 (1973).

(46) (a) G. A. Rodley and W. T. Robinson, *Nature (London)*, **235**, 438 (1972); (b) G. A. Rodley and W. T. Robinson, *Synth. Inorg. Met.-Org. Chem.*, **3**, 387 (1973); J. P. Collman, H. Takaya, B. Winkler, L. Libit, S. K. Seah, G. A. Rodley, and W. T. Robinson, *J. Am. Chem. Soc.*, **95**, 1656 (1973).

(47) R. S. Gall, J. F. Rogers, W. P. Schaefer, and G. G. Christoph, *J. Am. Chem. Soc.*, **98**, 5135 (1976).

(48) We might note here again that the general Walsh diagram of Figure 7 is uncertain with respect to level spacings. For instance in $\{MOO\}^6$ one might suspect a linear geometry and a low-spin ground state, yet $Cr(O_2)(py)(TPP)$ has two unpaired electrons: C. A. Reed, Abstracts, 172nd National Meeting of the American Chemical Society, San Francisco, Calif., 1976, No. INOR 125.

(49) D. M. P. Mingos, W. T. Robinson, and J. A. Ibers, *Inorg. Chem.*, **10**, 1043 (1971).

(50) W. R. Scheidt and J. L. Hoard, *J. Am. Chem. Soc.*, **95**, 8281 (1973).

(51) G. Broden, T. N. Rhodin, C. Brucker, R. Benbow, and Z. Hurych, *Surf. Sci.*, in press.

(52) R. Hoffmann, *J. Chem. Phys.*, **39**, 1397 (1963); R. Hoffmann and W. N. Lipscomb, *ibid.*, **36**, 2179, 3489 (1962); **37**, 2872 (1962).

(53) J. W. Lauher and R. Hoffmann, *J. Am. Chem. Soc.*, **98**, 1729 (1976).

# Seven-Coordination. A Molecular Orbital Exploration of Structure, Stereochemistry, and Reaction Dynamics

ROALD HOFFMANN,* BARBARA F. BEIER, EARL L. MUETTERTIES,* and ANGELO R. ROSSI

A systematic molecular orbital analysis of seven-coordinate molecules is presented, with an emphasis on the basic electronic structure, substituent site preferences, and pathways for interconversion of various geometries. Conformations studied in detail include the pentagonal bipyramid (PB), capped octahedron (CO), and capped trigonal prism (CTP). With respect to σ or electronegativity effects the following conclusions are reached for the optimum site of substitution in a $d^4$ complex by a better σ donor: PB equatorial (eq), CO capping site (c), CTP edge (e). For π effects the following preferences are deduced for $d^4$ systems substituted by an acceptor and $d^0$ by a donor (> means preferred): PB ax > eq, $eq_\parallel$ > $eq_\perp$; CO (cf = capped face, uf = uncapped face, c = capping site) cf > c > uf, $cf_\perp$ > $cf_\parallel$, $uf_\perp$ > $uf_\parallel$; CTP (qf = quadrilateral face, e = edge, c = capping site) qf ~ e > c, $qf_\perp$ > $qf_\parallel$, $e_\perp$ > $e_\parallel$, $c_y$ > $c_x$. These preferences are reversed for the $d^4$ donor substituent case. The agreement with information available from structural studies is good, though often the same conclusions would be reached from steric arguments. All pathways of polytopal rearrangement in seven-coordination are of low energy.

In the seemingly complex yet quite simply ordered[1] structural scheme for inorganic chemistry, seven-coordination occupies a niche that is formally analogous to five-coordination. Neither five- nor seven-coordinate complexes can achieve as meritorious a structural form as their nearest coordination neighbors, four, six, and eight; and consistently, each is a less common coordination form than their nearest neighbors. A partial explanation for the "discontinuties" at five- and seven-coordination may be derived from the graph shown in Figure 1. There is a much less effective packing arrangement in progressing from four- to five- or from six- to seven-coordination and a quite modest penalty in ligand repulsion effects for a return to a more uniform spatial array of ligands in a further progression from five- to six- (essentially no penalty) or seven- to eight-coordination.[2] Nevertheless, five[3,4] and seven-coordinate[5,6] complexes are isolable and well-defined molecular entities, although seven-coordination forms are by far the less common of the two presumably because of steric as well as electronic penalties incurred in the construction of

complexes of high coordination number. The role of seven-coordination is significant when viewed in the light of reaction intermediates or transition states in associative reactions of six-coordinate complexes, oxidative addition reactions of five-coordinate complexes, and, most importantly, dissociative reactions of eight-coordinate complexes. An understanding of mechanism in these reaction regimes requires delineation of the electronic and steric factors that direct structural and stereochemical trends in seven-coordination. This paper is addressed to the issue of electronic controls.

Structural studies[5,6] and calculations[7-10] suggest that seven-coordination has in the general[11] case a potential surface that is not distinguished by a deep minimum corresponding to one polytopal[12] form. This situation, analogous to that established for the five-coordination family, in part reflects the simple geometric fact that seven points cannot be arranged so as to describe a regular polyhedron. The number of nonisomorphic polyhedra with seven vertices is large, 34. Each of these polyhedra has been illustrated by Britton and Dunitz.[13] Within this complete set, just three high-symmetry polyhedra[5,6,14] suffice to describe the established elements of

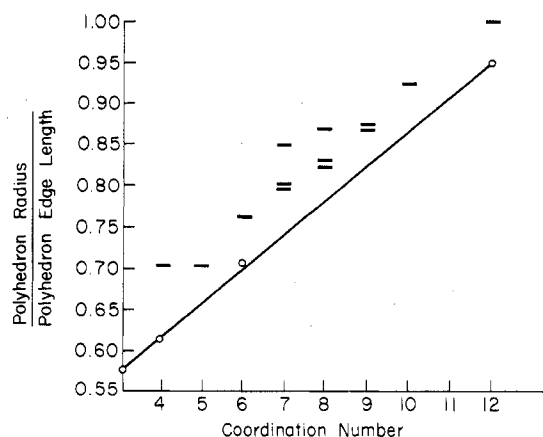* To whom correspondence should be addressed at Cornell University.

**Figure 1.** A plot of the ratio of polyhedron radius (M–L) to polyhedron edge length (L–L) vs. coordination number, $N$ (ML$_N$), for the various types of polyhedra, following the Day and Hoard discussion.[2a] The solid line representing optimal packing joins the points for the three regular polyhedra that have all faces triangular. Identification of specific polyhedra reading up for increasing ratio, i.e., less effective packing: $N$ = 4, the regular tetrahedron and the square; $N$ = 5, the trigonal bipyramid and (coincidentally) the tetragonal pyramid; $N$ = 6, the regular octahedron and the trigonal prism; $N$ = 7, the $C_{3v}$ monocapped octahedron, the $C_{2v}$ monocapped trigonal prism, and the $D_{5h}$ pentagonal bipyramid; $N$ = 8, the $D_{4d}$ square antiprism, the $D_{2d}$ dodecahedron, and the cube; $N$ = 9, the $D_{3h}$ tricapped trigonal prism and the $C_{4v}$ monocapped square antiprism; $N$ = 10, the $D_{4d}$ bicapped square antiprism; $N$ = 12, the regular icosahedron and the $O_h$ cuboctahedron.

structure[5,6] in seven-coordination although minor polyhedral variants of lower symmetry are useful for an accurate assessment of the more subtle structural details.

A constructive generation of the idealized seven-coordinate structures is the addition of a vertex (ligand) to the regular octahedron, a formal process analogous to the initial phase of an associative substitution reaction of a six-coordinate complex. Vertex addition along an octahedral edge, **1**, accompanied by a minor motion of four vertices coplanar with the new vertex, generates the $D_{5h}$ pentagonal bipyramid **2**.
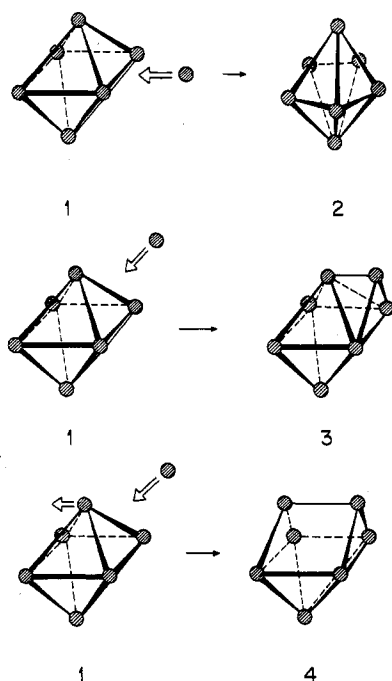


Face attack may generate either the $C_{3v}$ capped octahedron **3** or the $C_{2v}$ capped trigonal prism **4**. The latter is very closely related to the "trapezoidal octahedron" or "octahedral wedge"
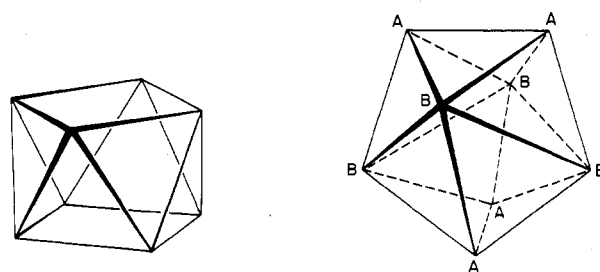


**Figure 2.** The two most common polyhedra in eight-coordination. On the left is the $D_{4d}$ Archimedean square antiprism and on the right the $D_{2d}$ dodecahedron. All vertices are equivalent in the former polyhedron whereas there are two types of vertices (A and B), distinguished by symmetry and connexity, in the dodecahedron.

which has been discussed as one possible way-point[15,16] in an associative ML$_6$ substitution reaction—the other possible transition state in a concerted reaction is the pentagonal bipyramid.[16b]

Alternatively, the idealized seven-coordinate forms **2–4** may be conceptually generated by vertex removal from the favored or most common[18] eight-coordinate geometries (see Figure 2). Although this approach is not readily envisaged nor readily illustrated by drawings (a careful inspection of models is required), there is a cogent reason for considering such a generation scheme. Seven-coordinate intermediates will be much more common in substitution reactions of eight-coordinate than of six-coordinate complexes. Starting from the $D_{2d}$ dodecahedral eight-coordinate form, there are two possible degradative processes because of the two different types of vertices (Figure 3). Vertex elision at an A site directly yields the $C_{3v}$ capped octahedron, **3**, although with minor displacements of the other vertices either the $D_{5h}$ (**2**) or $C_{2v}$ (**4**) forms may be generated. Removal of a B vertex gives a form closely related to the pentagonal bipyramid (**2**).[2b] Starting with the $D_{4d}$ square antiprism, removal of a vertex generates a structure that is closely related to the capped trigonal prism **4** by a minor relaxation of the other vertices and again to the other forms (**2** and **3**) by slightly larger displacements of the other vertices.

There is an endless array of variants for **2**, **3**, and **4** of which possibly the most important are directly generated from the $D_{5h}$ pentagonal bipyramid by out-of-plane motions of the vertices in the relatively cramped pentagonal girdle as shown for **5** ($C_s$) and **6** ($C_2$) which combined with the symmetric and
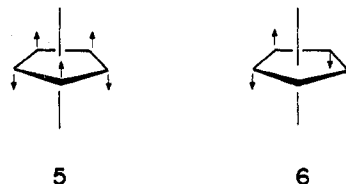


antisymmetric axial bending modes can not only generate the $C_s$ and $C_2$ polytopal forms but also describe the pathways for interconversion of the three high-symmetry seven-coordinate forms. Forms **5** and **6** were first identified by Bartell and Thompson[10] in calculations based on the valence-shell electron-pair repulsion model (VSEPR). They examined seven points constrained to move on the surface of a sphere and subject to a repulsive force $\sum_{i \neq j} r_{ij}^{-n}$, where $r_{ij}$ is the distance between two of the points. For $n < 2.5$, that is soft potentials, the preferred geometry was $D_{5h}$. For $2.5 < n < 5$ the lowest energy structures were the $C_s$ and $C_2$ forms **5** and **6** which merged into the $C_{2v}$ capped trigonal prism at $n \approx 5$. For $n > 5.6$ the capped octahedron $C_{3v}$ was the preferred conformation. In the range of low $n$, there was little difference in energy between any of the structures. Other variants that may be relevant only to seven-coordinate complexes with stereo-
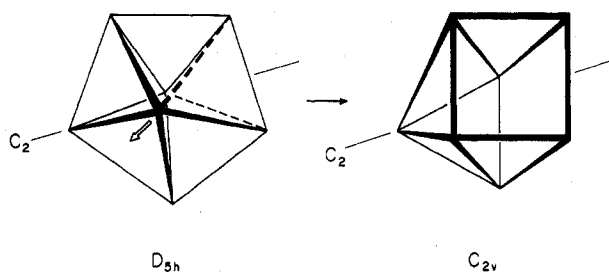
**Figure 3.** A representation of the interconversion of the $D_{5h}$ pentagonal-bipyramidal and $C_{2v}$ capped trigonal-prismatic geometries. The dotted lines in the $D_{5h}$ form represent the edges that are "lost" in the diamond to square face transition from $D_{5h}$ to $C_{2v}$. All forms between the $D_{5h}$ and $C_{2v}$ limits have $C_2$ symmetry and this common axis is denoted in the limiting geometries.
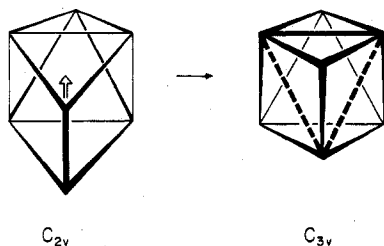


**Figure 4.** A stylized representation of the interconversion of the $C_{2v}$ capped trigonal-prismatic and $C_{3v}$ capped octahedral geometries. All forms intermediate between the $C_{2v}$ and $C_{3v}$ limits have a mirror plane which in the representation is vertical and normal to the plane of the paper. In this interconversion, the square (or really rectangular) faces in $C_{2v}$ are converted into diamond faces in $C_{3v}$. The dotted lines in the figure to the right represent the new "diamond" edges.

chemically constrained polydentate ligands or to special solid-state electronic or packing factors are the family of square base–trigonal cap polyhedral forms, of which one of the two $C_s$ forms is represented by **7**, and the $C_{3v}$ capped trigonal prism



**7**     **8**
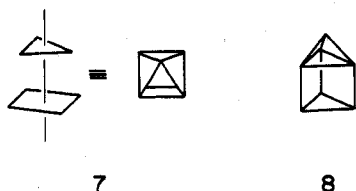
**8.**
There is a strikingly close relationship between the three high-symmetry idealized seven-coordinate forms, again a feature common to five-coordination. This phenomenon, best appreciated by the examination of stick (d-Stix[18]) models, is illustrated in Figures 3–5 for the $D_{5h} \rightleftarrows C_{2v}$, $C_{2v} \rightleftarrows C_{3v}$, and $D_{5h} \rightleftarrows C_{3v}$ interconversions.[6,19] Each of these has the stylized diamond face $\rightleftarrows$ square face[19a] interconversion form, a feature that is readily discerned in the perspectives of Figures 3–5, and each has a reaction path of forms that have a mirror plane except the $D_{5h}$–$C_{2v}$ traverse where intermediate forms may have $C_2$ or $C_s$ symmetry. The interconversions illustrated in Figures 3–5 represent only one of many possible physical motions that may describe each interconversion. Because of the relatively amorphous potential surface for seven-coordination, there may well be several different "physical" or geometric reaction paths for each type of interconversion, e.g., $D_{5h} \rightleftarrows C_{2v}$, which differ very little in terms of activation parameters. Because of the very small bending–stretching modes required to effect interconversions like those outlined in Figures 3–5, stereochemically nonrigid structures should be common in seven-coordination.[19b,c]
In the next section we begin a systematic molecular orbital exploration of various seven-coordinate geometries, supple-
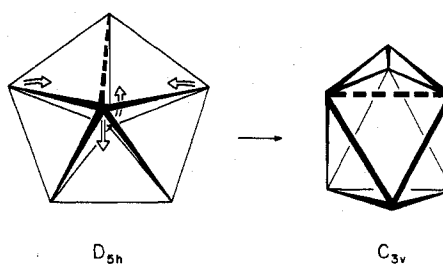


**Figure 5.** A possible mode for interconversion of the $D_{5h}$ pentagonal-bipyramidal and $C_{3v}$ capped octahedral geometries. All forms intermediate between the symmetry-defined limits have a mirror plane which is vertical in this perspective and normal to the plane of the paper. The dotted line edge in the $D_{5h}$ drawing is "lost" in the traverse, to be replaced by the orthogonal diamond edge shown in dotted outline for $C_{2v}$.

menting previous MO studies in the literature.[15,16,20] The emphasis is on an understanding of substituent site preferences and the pattern of bond strengths in this important class of molecules. We proceed along the lines of our previous analysis of five-coordination,[21] using extended Hückel calculations described in the Appendix.

**The Basic Seven-Coordinate Geometries**
There is an unavoidable complication in the discussion of the various seven-coordinate structures and their interconversions. A natural coordinate system exists for each structure—for instance, the $z$ axis as the vertical axis in **2** and **4** as drawn. However, the easy interconversion modes which connect these structures[5,6] are such that they do not preserve this symmetry axis. We begin by discussing the orbitals of each of the primary structures in its natural coordinate system. In the spirit of attempting to dissect out $\sigma$ and $\pi$ effects, the initial discussion is of a hypothetical $ML_7$ system where L is a pseudoligand bearing a single $\sigma$ orbital and two electrons.
**Pentagonal Bipyramid.** Illustration **9** shows the familiar
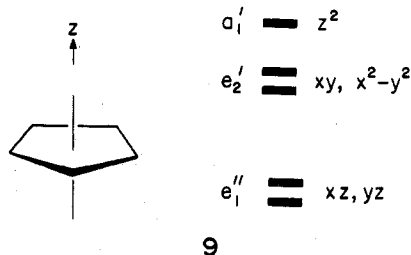


**9**

level pattern for this molecule.[16,20f] A low-lying $e_1''$ ($xz$, $yz$) does not mix in any ligand character at all. Relatively high above it lie the two metal–ligand $\sigma$-antibonding combinations $e_2'$ ($xy$, $x^2 - y^2$) and $a_1'$ ($z^2$). The level pattern resembles that of five-coordination except that in the present case the second e set, $e_2'$, is at much higher energy. The reason for this is that, unlike in the case of five-coordination, there is no metal p orbital set which can interact in symmetry-allowed fashion with these d orbitals and stabilize them. The population analysis for this structure is shown in **10**. It applies to any species with



**10**
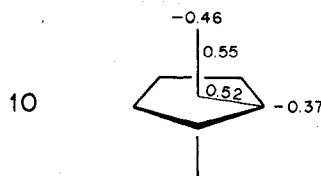
0–4 d electrons. The implication is that as far as $\sigma$ bonding is concerned the axial bonds should be marginally stronger. At first sight this conclusion appears to contrast with the trigonal-bipyramid case in five-coordination. There the axial bonds were weaker for a phosphorane or a $d^0$ or $d^{10}$ transition

**Table I.** $ML_7$ Structures

| Species | Config'n | Structure | Ref |
|---|---|---|---|
| $IF_7$ | $d^{0\ a}$ | $D_{5h}$ | 23 |
| $ZrF_7{}^{3-}$ | $d^0$ | $D_{5h}$ | 24 |
| $NbF_7{}^{2-}$ | $d^0$ | $C_{2v}$ | 25 |
| $ReF_7$ | $d^0$ | $D_{5h}$ | 26 |
| $V(CN)_7{}^{4-}$ | $d^2$ | $D_{5h}$ | 27 |
| $Mo(CN\text{-}t\text{-}Bu)_7{}^{2+}$ | $d^4$ | $C_{2v}$ | 28 |
| $Mo(CN)_7{}^{5-}$ | $d^4$ | $D_{5h}$ | 29 |

$^a$ Or $d^{10}$.

metal complex. This was understandable from a Rundle model[22] of normal equatorial and electron-rich three-center axial bonding. In the present case one could retain the three-center model for the axial bonding, but one is forced into a delocalized multicenter electron-deficient bonding scheme for the five equatorial bonds as well. This is because the three central-atom s and p orbitals in the equatorial plane transform as $a_1' + e_1'$, while the five equatorial ligand donor orbitals are $a_1' + e_1' + e_2'$. Only three fully bonding combinations result—the $e_2'$ ligand set is nonbonding until we allow mixing with the metal d orbitals. That mixing enhances equatorial bonding but apparently not to the extent of making those bonds stronger than the axial ones.

Known $ML_7$ structures are summarized in Table I. Prior to consideration of $\pi$-bonding effects it may be premature to point to any structural trends. The accuracy of some of the structures is limited. Among those which are $D_{5h}$, or close to that limit, we have $V(CN)_7{}^{4-}$, with nearly equal V–C distances, and $IF_7$, which has a distinctly shorter axial I–F bond. Shorter axial distances are typical of U(IV) PB complexes with oxygens in both axial and equatorial sites,[30a] although, in these uranyl complexes, it is very likely that $\pi$ bonding along the axis is responsible for this difference.

A consequence of the $ML_7$ charge distribution shown in **10**, with apical ligands distinctly more negative, is that one would anticipate that more electronegative ligands, better $\sigma$ acceptors, should preferentially enter the axial sites. Better $\sigma$ donors should favor the equatorial sites. This is for $d^0$–$d^4$ complexes. Were the number of d electrons to surpass 4, these conclusions would be modified. Cases where $\sigma$ effects alone are dominant are rare, but one such may be $H_4Os(PMe_2Ph)_3$. The better $\sigma$-donor hydrides are all equatorial.[30b]

**Capped Octahedron.** Within the $C_{3v}$ constraint and with equal M–L distances this 1:3:3 partition retains two degrees of freedom. These may be chosen as the spherical angles $\theta_2$ $(=\theta_3 = \theta_4)$ and $\theta_5$ $(=\theta_6 = \theta_7)$ characterizing the two triangles in **11**. The capped regular octahedron, $\theta_2 = 54.7°$, $\theta_5 =$



11
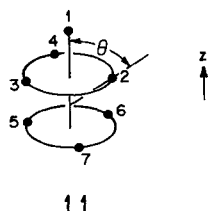
$125.3°$, is clearly congested. The calculations of Thompson and Bartell[10] yield a relatively narrow range of optimal geometries progressing from $\theta_2 = 73.3°$, $\theta_5 = 128.8°$ for $n = 1$ to $\theta_2 = 75.8°$, $\theta_5 = 131.4°$ for $n = 12$ ($n$ is the power in the repulsive potential). These values are not very different from $\theta_2 = 75°$, $\theta_5 = 130°$, which is what our molecular orbital calculation gives for $L_7{}^{7-}$, that is, seven ligands on a sphere without a central metal atom. If we insert the metal atom, we get for the $d^0$ configuration $\theta_2 = 84°$, $\theta_5 = 138°$; for low-spin $d^2$ $\theta_2 = 80°$, $\theta_5 = 130°$; for $d^4$ $\theta_2 = 70°$, $\theta_5 = 130°$. An earlier MO calculation by Gavin[20c] for the specific case of $IF_7$ gave $\theta_2 = 75°$, $\theta_5 = 127°$.

The MO results agree well with the VSEPR predictions. The slight trend that is noted is that $\theta_2$ and $\theta_5$ both decrease as the number of d electrons is increased from 0 to 4. This can be understood from the level scheme for the capped octahedron. Illustration **12** shows the d-block splitting pattern



12
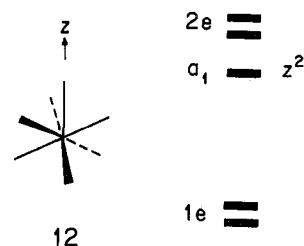
for a typical geometry, $\theta_2 = 75°$, $\theta_5 = 130°$. The $a_1$ orbital metal contribution is nearly all $z^2$, while the e orbitals are linear combinations of $(xy, x^2 - y^2)$ and $(xz, yz)$, with some admixture of $x$ and $y$. Imagine the approach of a capping ligand to an octahedral face. The $O_h$ levels reduce in the resultant $C_{3v}$ symmetry as follows: $t_{2g} \rightarrow a_1 + e$, $e_g \rightarrow e$. If the incoming seventh ligand bears only a $\sigma$ orbital, then it interacts exclusively with the $a_1$ component of $t_{2g}$, destabilizing it.

The ligand–ligand repulsions, which make $\theta_2$ and $\theta_5$ greater than the regular octahedron values, can be found in the bonding molecular orbitals below the d block. The deformation which optimizes the total energy of the $d^0$ configuration actually has destabilized the 1e levels. That orbital set would be completely nonbonding in the regular octahedron. It does not interact with the incoming ligand directly, but indirectly the steric distortion pushes the six ligands into slight $\sigma$-antibonding positions relative to the metal d orbitals. Any deformation which would lead back toward the octahedron, i.e., lowering $\theta_2$ toward $54.7°$ and $\theta_5$ toward $125.3°$, would increase the energy of the lower lying $\sigma$ levels and would stabilize 1e. This is why $d^2$ and $d^4$ move to lower $\theta_2$ and $\theta_5$ relative to $d^0$. We should note that the slight geometrical trend we discuss for $ML_7$ is greatly attenuated if the ligand L is made a more realistic ligand like chloride. For $MCl_7$ we calculate an optimum $\theta_2 = 75°$, $\theta_5 = 130°$ for both $d^0$ and $d^4$ configurations.

A population analysis for the capped octahedron, $d^4$, is shown in **13**. The $d^0$ case differs only by having less electron



13
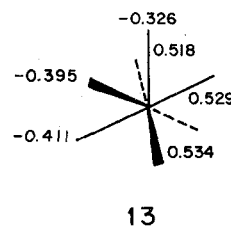
density in both triangles. We would conclude that as far as the $\sigma$ effect is concerned the weakest bond should be to the capping ligand for $d^4$. The better $\sigma$ donors should preferentially enter the capping site in $d^0$–$d^4$.

There are no capped octahedra among the $ML_7$ structures, but there are several in the list of $ML_xL'_yL''_z$, mixed-monodentate-ligand crystal structures that is given in Table II. The two $d^2$ structures all have $\theta_2$ near 74–75° and $\theta_5$ near 127°. For some of the $d^4$ structures we do not have the required information; others are distorted toward the CTP geometry. If we ignore the asymmetries and simply average the angles, we get values such as 71.9, 128.6° for $MoCl_2(CO)_2P_3$,[41] 73.2, 125.6° for $W(CO)_3P_3I^+$,[40] and 72, 128° for $WBr_2(CO)_3As_2$.[43] In the more symmetrical $W(CO)_4Br_3{}^-$ the angles are 74.1, 125.5°. No significant trend is visible. We noted above that the calculated $ML_7$ trend with L a model $\sigma$ ligand was very much diminished for L = Cl.

**Table II.** Structures of the $ML_xL'_yL''_z$ Type, with Seven Mixed Monodentate Ligands

| Complex[a] | $x$ in $d^x$ | Struc-ture[b] | Ref | Geometrical details[c] |
|---|---|---|---|---|
| $UO_2F_5^{3-}$ | $0^d$ | PB | 31 | O:FFFFF:F |
| $NbOF_6^-$ | 0 | PB | 32 | F:FFOFF:F |
| $UO_2(urea)_4(H_2O)$ | $0^d$ | PB | 33 | O:OOOOO:O |
| $UO_2(NCS)_5^{3-}$ | $0^d$ | PB | 34 | O:NNNNN:O |
| $UCl(tmpo)_6^{3+}$ | $0^e$ | CO | 35 | Cl:OOO:OOO |
| $MoCl_4P_3$ | 2 | CO | 36 | Cl:PPP:ClClCl; $\theta_2 = 74.6°, \theta_5 = 127.2°$ |
| $MoBr_4P_3$ | 2 | CO | 37 | Br:PPP:BrBrBr; $\theta_2 = 74.5°, \theta_5 = 127.4°$ |
| $W(CO)_4Br_3^-$ | 4 | CO | 38 | C:CCC:BrBrBr; $\theta_2 = 74.1°, \theta_5 = 125.5°$ |
| $Mo(CNR)_6I^+$ | 4 | CTP | 39 | I:CCCC:CC |
| $W(CO)_3P_3I^+$ | 4 | CO/CTP | 40 | as CO P:CCC:PPI as CTP I:CCPP:CP |
| $MoCl_2(CO)_2P_3$ | 4 | CO/CTP | 41 | as CO C:CPP:PClCl as CTP Cl:CPPCl:PC |
| $MoCl_2(CO)_3P_2$ | 4 | CO | 42 | C:CCP:PClCl |
| $MoBr_2(CO)_2P_3$ | 4 | CO | 42 | C:PPP:CBrBr |
| $WBr_2(CO)_3As_2$ | 4 | CO | 43 | C:CCAs:AsBrBr |

[a] P = phosphine, As = arsine, R = alkyl. [b] Where two structures are indicated, the geometry is intermediate. [c] Partitioning of ligands is indicated in an obvious way: 1:5:1 for PB, 1:3:3 for CO, 1:4:2 for $C_{2v}$ CTP. [d] U(VI). [e] U(IV).

The 1:3:3 partition of a capped octahedron points to another natural construction of level scheme **12**. This is by interacting a $C_{3v}$ $XMY_3$ fragment with three additional ligands, a procedure that has already been implemented.[44]

**Capped Trigonal Prism.** The capping ligand can enter a triangular or a tetragonal face of the trigonal prism, giving rise to a $C_{3v}$ or $C_{2v}$ geometry, **8** or **4**. The former has not been discussed in the literature, perhaps because there appear to be no known examples,[45] perhaps because of a feeling that such a structure would be very crowded. We have not optimized this $C_{3v}$ geometry but have simply rotated the lower triangle of the capped octahedron so that it lies directly under the upper triangle. The resultant level scheme **14** once again shows an



**14**
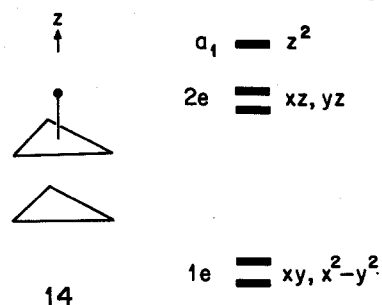
e orbital at low energy, $a_1 + e$ high up. These levels are most easily derived by bringing in a capping ligand onto a trigonal prism. The $D_{3h}$ structure has low-lying $a_1' + e'$ and high-energy $e''$.[46] A ligand approaching along the $z$ axis interacts strongly with $z^2$, destabilizing it.

The difference between the two $C_{3v}$ forms, capped octahedron vs. capped trigonal prism, is in the energy of the lower e orbital. This level is unaffected by the capping, differing little from $e'$ in $D_{3h}$ or a component of $t_{2g}$ in $O_h$. The lower e level is at higher energy in the capped trigonal prism, for there is some antibonding between $xy$, $x^2 - y^2$ and ligand $\sigma$ functions that is absent in the octahedron.[46] Thus the $C_{3v}$ CTP is especially destabilized relative to the $C_{3v}$ CO for the $d^4$ configuration. For the $d^0$ configuration, e unoccupied, the situation changes. We in fact find the $C_{3v}$ CTP more stable than the $C_{3v}$ CO. A similar effect occurs in the uncapped $ML_6$ structures,[46] and here as there we are not certain if the effect is real or if it is an artifact of the extended Hückel procedure.

**Table III.** $C_{2v}$ Capped Trigonal Prism Parameters[a]

| Structure | | $\theta_2$, deg | $\varphi_2$, deg | $\theta_6$, deg |
|---|---|---|---|---|
| Points on a sphere[b] | $n = 1$ | 80.8 | 49.0 | 144.2 |
| | $n = 6$ | 79.4 | 48.7 | 143.3 |
| | $n = 12$ | 78.3 | 48.7 | 142.6 |
| Calcd $L_7^{7-}$ | | 79 | 48 | 142 |
| $ML_7$ $d^0$ | | 68 | 52 | 118 |
| $ML_7$ $d^2$ | | 80 | 54 | 122 |
| $ML_7$ $d^4$ | | 82 | 46 | 148 |
| $MCl_7$ $d^0$–$d^4$ | | 80 | 48 | 145 |
| $M(CO)_7$ $d^4$ | | 85 | 48 | 150 |
| $NbF_7^{2-}$ [c] $d^0$ | | 78.6 | 48 | 143.0 |
| $Mo(CN-t-Bu)_7^{2+}$ [d] $d^4$ | | 82.0 | 50 | 144.0 |

[a] The last two entries are experimental structure determinations. [b] Reference 10. [c] Reference 25. [d] Reference 28.

The trigonal prism capped on a tetragonal face, **4**, has received considerably more attention. The structural type is observed in $NbF_7^{2-}$ and $Mo(CN-t-Bu)_7^{2+}$ (see Table I) as well as in complexes with several more complicated ligand sets.[5] If equal ML bond lengths are assumed, the structure may be described by three independent polar angles:[10] $\theta_2$ ($=\theta_3 = \theta_4 = \theta_5$), $\varphi_2$ ($=-\varphi_3 = 180° + \varphi_4 = 180° - \varphi_5$), and $\theta_6 = \theta_7$ ($\varphi_6 = 0°, \varphi_7 = 180°$). Note that $\varphi_2$ is not constrained to 45°; i.e., we do not require that the capped face of the trigonal prism be square.

Table III lists the Thompson and Bartell optimum geometries for $n = 1$, 6, and 12, our computed minima for several $d^n$ configurations and seven ligands alone, as well as the related parameters of the two observed $ML_7$ structures. Our $L_7^{7-}$ and $ML_7$ (L is a pseudoligand bearing a single s-type orbital) $d^4$ cases are in good agreement with the observed structures and the VSEPR calculation. This is not so for the calculated $d^0$ geometry. However, when we optimized a more realistic $MCl_7$ structure, the $d^0$ case gave $\theta_2 = 80°$, $\varphi_2 = 48°$, and $\theta_6 = 145°$.

The molecular orbitals of a model $C_{2v}$ CTP structure, corresponding to the points on a sphere optimal geometry with $n = 6$, are shown in **15**. There are some minor discrepancies



**15**
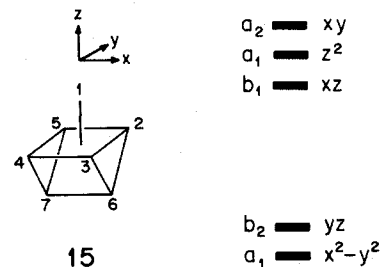
between this level ordering and that deduced by other workers[15,16,20d,f,47] from a crystal field model, but that may be due to differing assumptions about geometries. The levels are once again easily derived from those of a trigonal prism.[46] The level ordering in $D_{3h}$ is $a_1'$ ($x^2$) $< e'$ ($yz, y^2 - z^2$) $<<$ $e''$ ($xz$, $xy$). The d levels are those appropriate to the geometrical situation at hand, namely, the $x$ axis being the threefold axis of the trigonal-prism fragment. The group theoretical reduction is $a_1' \rightarrow a_1$, $e' \rightarrow a_1 + b_1$, $e'' \rightarrow a_2 + b_1$. The capping ligand is $a_1$ and interacts with the "$y^2 - z^2$" component of $e'$ as well as with "$x^2$". These $a_1$ orbitals mix so that the lower $a_1$ becomes primarily $x^2 - y^2$ and the upper, destabilized one, $z^2$.

Note that for the first time we encounter a splitting of the two lowest levels. This is potentially an interesting phenomenon, for, if the splitting were large, a $d^2$ $ML_7$ complex might have a chance of having a low-spin ground state. In the geometry we calculated, however, the splitting of $a_1$ and $b_2$ is small, 0.16 eV. The CTP structure has been inferred for $d^3$ $Mo(CN)_7^{4-}$ [20d] and $d^1$ $Ti(CN)_7^{4-}$.[48] Electron spin resonance studies aimed at detecting the symmetry of the orbitals oc-

cupied in these molecules would be of great interest.

Our calculations show an interesting trend on filling the lower d levels: an increase in $\theta_2$ and $\theta_6$, a slight decrease in $\varphi_2$. To understand this behavior consider the relevant $a_1$ ($x^2 - y^2$) and $b_2$ ($yz$) levels, drawn in **16** and **17**. The $a_1$, **16**, level
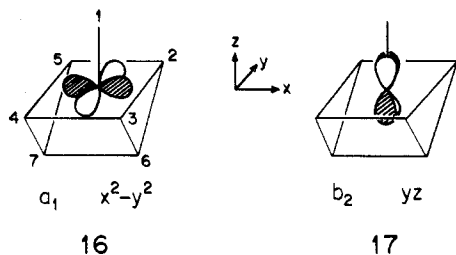


interacts with all ligands but most strongly with the unique edge 6-7. If $\theta_6 = \theta_7$ were to decrease, the metal–ligand, $\sigma$-antibonding character in $a_1$ would be enhanced. Therefore the larger $\theta_6$, the lower the energy of the $a_1$. Minimum antibonding with atoms 2, 3, 4, and 5 is also ensured by keeping $\varphi_2$ near 45°. The $b_2$ orbital **17** has mixed into it only the tetragonal-face ligand orbitals. The greater $\varphi_2$, the more $\sigma$ antibonding. Similarly, maximum $\sigma$ antibonding would occur at $\theta_2 = 45°$. Thus occupation of the $b_2$ orbital would favor a larger $\theta_2$ and a smaller $\varphi_2$.

The electron distribution in the CTP geometry for $d^0$ and $d^4$ configurations is illustrated in **18**. There is little relative
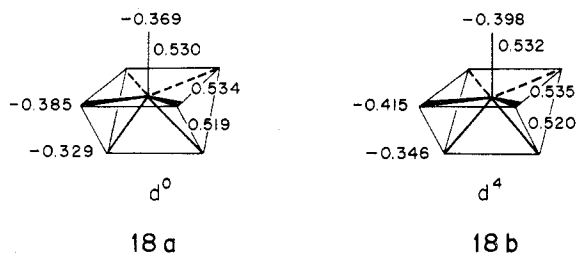


change in the overlap populations and net charges as one goes from $d^0$ to $d^4$. In either case the weaker bonds are to the lower edge. Populating the $a_1$ and $b_2$ orbitals adds electron density to all ligands. In both $d^0$ and $d^4$ the better $\sigma$ donors should enter the more positive sites on the unique edge.

**Trigonal Base–Tetragonal Base.** As we noted earlier, this is really a family of structures in which a set of four tetragonal or square vertices in a plane rotates against a trio of points in a parallel plane. Along the rotation itinerary 24 structures of $C_s$ symmetry are encountered: 12 of type **19**, 12 of type
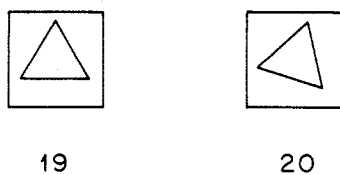


**20.**

We carried out a limited geometry optimization on **20**, assuming square and equilateral triangle faces. This resulted in a geometry with $\theta_1$ ($=\theta_2 = \theta_3$) = 50°, $\theta_4$ ($=\theta_5 = \theta_6 = \theta_7$) = 120° for $d^4$ ML$_7$, MCl$_7$, and M(CO)$_7$. This ML$_7$ geometry was then simply rotated into **19**. Not unexpectedly the 12-fold barrier was minute. Type **20** was more stable by 0.002 kcal/mol. The level scheme in these structures is normal, two orbitals down and three up in energy, and the charge distributions only reveal the geometrical similarity to some of the other limiting structures.

**General Features.** The previous sections have examined in some detail the electronic structure of several of the higher symmetry ML$_7$ structures. Some lower symmetry structures, for instance **7** and **8**, have been calculated but not described.
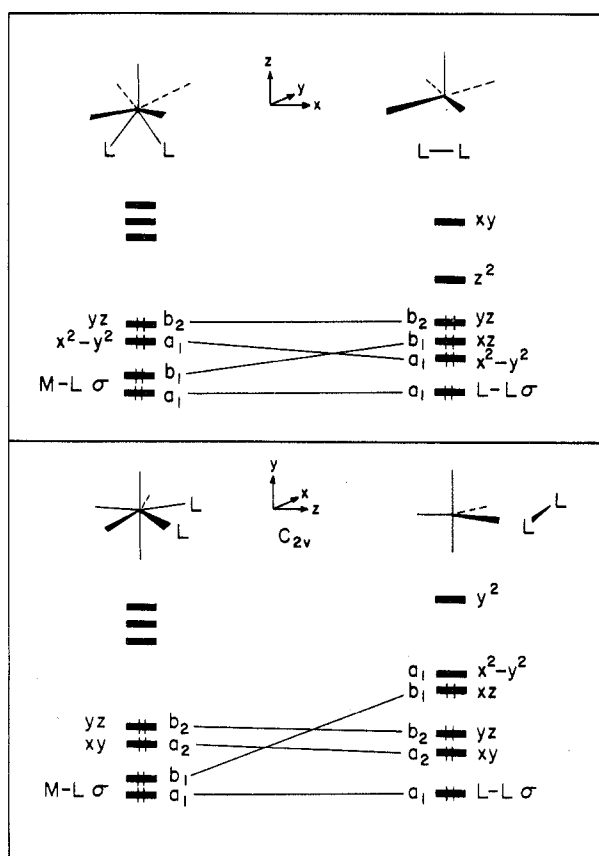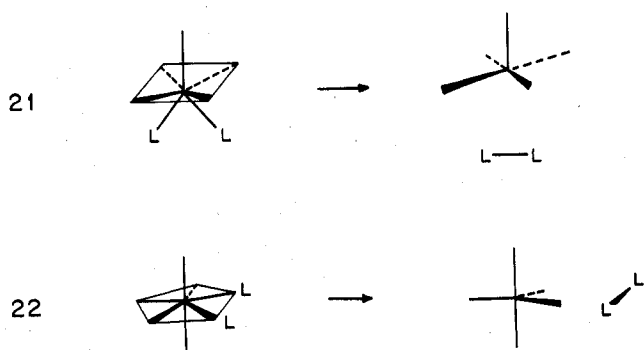
**Figure 6.** Correlation diagrams for the concerted elimination of two ligands from a capped trigonal prism leading to a square pyramid (top) and from a pentagonal bipyramid leading to a trigonal bipyramid (bottom). Not all levels are indicated in the diagram, but only the crucial metal–ligand bonding levels and the d block. Correlations are drawn only between the occupied levels. Note that in the bottom diagram the coordinate system, appropriate to the $C_{2v}$ symmetry maintained, is an unconventional one for both reactant and product.

Their levels and electronic distributions resemble those of the higher symmetry structures just as their geometries do.

One general feature which emerges from our calculation is the ubiquitous level pattern of two low-energy orbitals and three high-energy or destabilized ones. Two low-energy orbitals of course implies a large gap between filled and unfilled levels, a low-spin ground state, relative kinetic stability, and a resistance to second-order Jahn–Teller distortions only to $d^4$ complexes. Not surprisingly these are the ML$_7$ complexes that satisfy the 18-electron rule. They form by far the most numerous class of known seven-coordinate molecules, though there are several well-characterized series with more electrons.[49-51]

Another feature of the calculations, not mentioned in the individual discussions, is the existence of small positive overlap populations among some of the ligands, especially in the $d^4$ configuration. For example, the L–L population between the two ligands on the unique edge in the $C_{2v}$ CTP is 0.024 and between two adjoining ligands in the pentagonal girdle of the PB is 0.020. These numbers are small. However, our past experience with overlap populations between nonbonded atoms attached to carbon in organic molecules leads us to suspect that in the context of these relatively crowded molecules such positive overlap populations, as small as they are, may be indicative of attractive interactions.

One way to look at these positive bond orders is to consider them as incipient bonding interactions. Extending that notion, we are led to analyze the reductive elimination or fragmentation reactions **21** and **22**. Figure 6 shows correlation diagrams for these processes, assuming a least-motion $C_{2v}$ reaction

21



22

**Table IV.** Energies of Capped Octahedron, $C_{2v}$ Capped Trigonal Prism, and $C_s$ Trigonal Base-Tetragonal Base Structures Relative to the $D_{5h}$ Pentagonal Bipyramid

| | | Energy, kcal/mol | | | |
|---|---|---|---|---|---|
| | | $ML_7$ $d^4$ | $MCl_7$ $d^0$ | $d^4$ | $M(CO)_7$ $d^4$ |
| $D_{5h}$ | PB | [0] | [0] | | [0] |
| $C_{3v}$ | CO | 13 | 0 | 1 | 5 |
| $C_{2v}$ | CTP | 12 | 2 | 2 | 4 |
| $C_s$ | 3:4 | 16 | 11 | 9 | 7 |

path. Both are allowed reactions, though **22** leaves the $ML_5$ fragment in a low-spin $d^6$ $D_{3h}$ configuration, which almost certainly is an excited state for that geometry.[21a,44,52] A $d^6$ $D_{3h}$ molecule is likely to have a high-spin ground state. The low-spin configuration will distort to the square pyramid. In fact one can draw a correlation diagram going directly from the PB to a square-pyramidal $ML_5 + L_2$, and the result is a symmetry-allowed process. The reverse of reaction **21** is one mechanistic pathway invoked in some reactions of tungsten and molybdenum carbonyls.[53,54]

A recent study by Lam, Corfield, and Lippard[47b] has revealed a remarkable reductive coupling of the adjacent edge ligands in $MoL_6I^+$, L = *tert*-butyl isocyanide. The reaction may be promoted by the attractive interaction between the unique edge ligands.

**Polytopal Rearrangements**

Just as there are many possible geometries for seven points on the surface of a sphere, so there are many pathways for interconverting the various limiting forms. This point was made in the introduction, and several of the possible interconversion modes were shown in **5, 6,** and Figures 3–5. We have examined potential energy surfaces for these specific motions for $ML_7$, where L = pseudoligand, Cl, and CO. There was no geometry optimization along the reaction path but merely a progression simultaneously in all of the spherical coordinates from one structure to the other. Because of the low $C_2$ or $C_s$ symmetry of the reaction paths, the lower d-block levels, the ones occupied in the $d^4$ complexes, were split in energy. But they never split by much and always correlated smoothly from one structural limit to another. Consequently there were no significant barriers along any of the reaction paths. No level crossings were to be expected, at least for $d^0$–$d^4$ complexes—these are all symmetry-allowed reactions.

The only changes in energy along the rearrangement pathways were those caused by the calculated stability of the terminal structures. These we must discuss next. But before we do this we must remind the reader of two points. First, the limitations of the extended Hückel method for calculating isomer stabilities are nontrivial. Second, we have restricted ourselves to equal M–L distances. Each geometrical limit will adjust the M–L distances, and a calculation which assumes all such distances equal may not be a good guide to the actual stability.

With these cautionary points in mind we show in Table IV the calculated energies of three $d^4$ geometries of $ML_7$, $MCl_7$, and $M(CO)_7$ relative to the energy of the $D_{5h}$ structure. There are some interesting variations in the relative energies of the various structures depending on the donor or acceptor properties of the ligands. We will discuss these in detail in the next section, but at this point note that the similiarity in energy of the $d^0$ $MCl_7$ $D_{5h}$ and $C_{2v}$ structures that we calculate is supported by the structural data assembled in Table I. The known $d^0$ fluorides are pentagonal bipyramids in the solid state, except for $NbF_7^{2-}$ which is a capped trigonal prism. For a $d^4$ $M(CO)_7$ we calculate a 4-kcal/mol preference for a PB. The

observed $Mo(CN-t-Bu)_7^{2+}$, for which $M(CO)_7$ might have been thought to be a model, is however a CTP.[28] But another $d^4$ complex, $Mo(CN)_7^{5-}$, is a PB.[29]

As we mentioned above, there are no calculated barriers between these structures along pathways illustrated in Figures 3–5. Still further mobility in the system is introduced by the 3:4 structures **19** and **20**, which are closely related to the CTP, CO, and PB geometries or way-points between these. The low barrier to rotation in the 3:4 structures was noted earlier. Such low barriers are analogous to those for intermediates in the turnstile rotation mechanism proposed for five-coordination.[55]

**Site Preferences of $\pi$ Donors and Acceptors**

Interactions of the $\pi$ type may be probed in a number of ways. Either a test 2p orbital or a pair of them may be introduced on the pseudoligand L or actual models for $\pi$-acceptor or $\pi$-donor substituents, such as CO or Cl, can be used. Whichever probe is chosen one has a further alternative of focusing on the total energy, the energy of the specific substituent orbitals, or the overlap populations with the substituent as a measure of the extent of interaction. To some degree we have used all of these criteria in the subsequent discussion. We have also made a point of considering not only cylindrical $\pi$-interacting groups, bearing two $\pi$-donating orbitals as shown in **23**, but also "single-faced" $\pi$ systems,



23                    24

exemplified by $-NR_2$, $-NO_2$, and $C_2H_4$ and shown in **24**. Some of the most interesting orientational effects are anticipated for this class of single-faced $\pi$ systems.[21] We begin with a discussion of the limiting structures.

**Pentagonal Bipyramid.** The four possible orientations of a substituent orbital are shown in **25**. Reference to scheme **9**



25                    26                    27
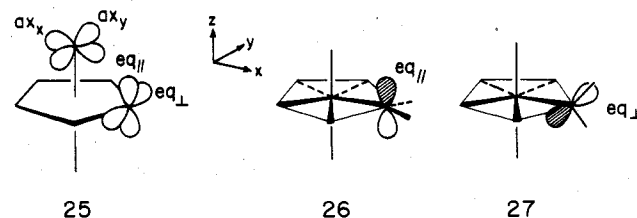
shows that the four d electrons enter the $e_1''$ level which is pure $xz, yz$. The interactions are thus ordered $ax_x = ax_y = eq_\parallel > eq_\perp$.[56] Before we draw the conclusions that follow from this ordering, we explore the alternative coordination geometries.

**Capped Octahedron and Capped Trigonal Prism.** The reason for considering these geometries together is that in both there are three distinct substitution sites: the apex, the capped face, and the uncapped face (CO) or unique edge (CTP). Let us denote these sites as c, cf, and uf in the CO and c, qf (quadrilateral face), and e (edge) in the CTP, following the notation introduced by Drew[5] (see **28** and **29**).
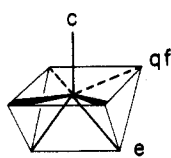
The natural coordinate system that we defined previously for these geometries is suitable for a capping ligand but not

**Table V.** Overlaps between a Substituent p Orbital and the Metal Orbital Interacting with It

| Capped octahedron | | Capped trigonal prism | |
|---|---|---|---|
| $c_x$ | 0.197 | $c_x$ | |
| $c_y$ | 0.197 | $c_y$ | 0.190 |
| $cf_\perp$ | 0.250 | $qf_\perp$ | 0.204 |
| $cf_\parallel$ | 0.174 | $qf_\parallel$ | 0.170 |
| $uf_\perp$ | 0.194 | $e_\perp$ | 0.190 |
| $uf_\parallel$ | 0.140 | $e_\parallel$ | 0.171 |
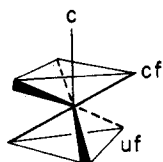


28  29

so for ligands occupying the other sites. For these we define a local coordinate system $(x', y', z')$ as follows: (1) Place the ligand on the positive $x'$ axis, i.e., the vector M–L is along $x'$. (2) Choose the $z'$ axis orthogonal to $x'$, and in the plane containing the apical M–L bond. (3) Let the $y'$ axis complete a right-handed coordinate system. The procedure is illustrated in **30** for the e site of a CTP. We then define as $\perp$ the
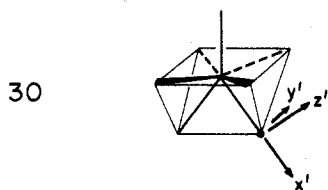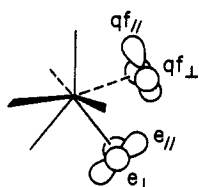


30

substituent p orbital along the $y'$ axis and as $\parallel$ the p orbital along $z'$. The parallel reference is to approximate parallel character to the principal $z$ axis. The various possible substituent orientations are drawn in **31** and **32**. In all cases
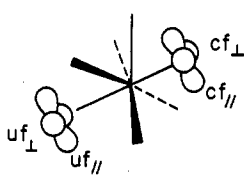


31  32

except the CTP qf sites the ML bond lies in a mirror plane and this separation is "clean"; that is, the $\parallel$ and $\perp$ orbitals cannot interact with each other and each p orbital interacts with different d orbitals.

The actual calculations were carried out with a single ligand bearing s and p orbitals and labeled as D ($\pi$ donor) or A ($\pi$ acceptor) dependent on the energy and occupation of the p orbitals. Details of the modeling are given in the Appendix. Also $CH_2^+$ and $NH_2$ were examined. The cases considered in detail were $d^0$ $ML_6D$, $d^4$ $ML_6D$, and $d^4$ $ML_6A$. We did not analyze $d^0$ $ML_6A$ because the metal d orbitals that would overlap with the empty ligand p orbitals are empty; hence the only interaction that the p orbitals of A would have will be with the filled $\sigma$-type orbitals, and this interaction is small. Moreover, there appear to be few $d^0$ $ML_7$ structures containing $\pi$-acceptor ligands.

In both the CO and CTP polytopes there are two low-lying d orbitals that can interact with p orbitals on the ligands. In the CTP case one of the orbitals is largely $x^2 - y^2$ and one is largely $yz$. These are drawn in **33** and **34**, and their primary interactions noted.
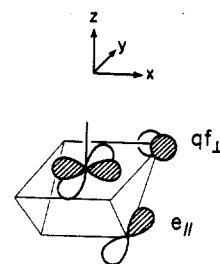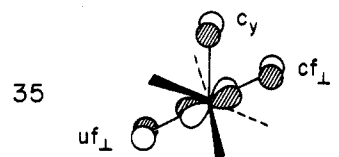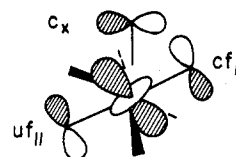


33
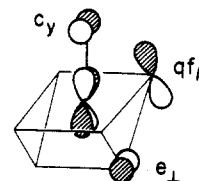
34

In the CO case the two d orbitals are mixtures of $xy$ and $yz$ and of $x^2 - y^2$ with $xz$, respectively. Their approximate shape is sketched in **35** and **36**. These diagrams indicate the



35

36

overlap possibilities. Just how good the interactions are depends on the relative values of the overlaps. Qualitative judgments are easy to make. Thus **35** and **36** imply that the $cf_\perp$ and $uf_\perp$ interactions should be greater than $cf_\parallel$ and $uf_\parallel$, respectively. Detailed comparisons are not so easy—for instance, the schematic drawing of orbital **35** does not reveal that the $cf_\perp$ interaction is significantly greater than $uf_\perp$. That is a consequence of the tilt of **35** and d–p hybridization which makes the orbital "point" better at a p orbital on a capped face substituent.

To facilitate the intercomparison of the various interactions we computed the overlaps between the metal orbitals (**33–36**) and a p orbital of a probe—a donor or acceptor at every distinct site.[57] Table V summarizes this information. Note the general superiority of $\perp$ interactions to $\parallel$ ones. For a ligand bearing two $\pi$-type orbitals, that is, a cylindrically symmetrical $\pi$ donor or acceptor, the capped octahedron provides maximum interaction in the capped face and minimal in the uncapped face. For the capped trigonal prism the quadrilateral face and edge are fairly well balanced and superior to the apical site, which by symmetry has a single interaction.

To proceed to the stage of actual predictions of substituent site preferences we must take into account the occupancy of the two d orbitals. The three cases we consider are shown schematically as
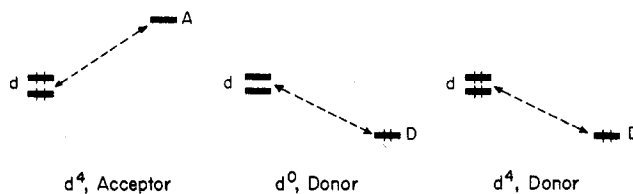


$d^4$, Acceptor  $d^0$, Donor  $d^4$, Donor

**Table VI.** Substituent Site and Orientation Preferences[a]

| | Pentagonal Bipyramid | | |
|---|---|---|---|
| $d^4$ A and $d^0$ D[b] | ax > eq | $eq_\parallel > eq_\perp$ | |
| $d^4$ D | eq > ax | $eq_\perp > eq_\parallel$ | |
| | Capped Octahedron | | |
| $d^4$ A and $d^0$ D | cf > c > uf | $cf_\perp > cf_\parallel$ | $uf_\perp > uf_\parallel$ |
| $d^4$ D | uf > c > cf | $cf_\parallel > cf_\perp$ | $uf_\parallel > uf_\perp$ |
| | Capped Trigonal Prism | | |
| $d^4$ A and $d^0$ D | qf ~ e > c. | $qf_\perp > qf_\parallel$ | $e_\perp > e_\parallel$ | $c_y > c_x$ |
| $d^4$ D | c > qf ~ e | $qf_\parallel > qf_\perp$ | $e_\parallel > e_\perp$ | $c_x > c_y$ |

[a] The symbols are defined in the text. > means preferred, at lower energy. [b] A = $\pi$ acceptor; D = $\pi$ donor.

The first two are basically the same—if the d orbitals are filled and the substituent is an acceptor or if the d orbitals are empty and the substituent a donor, in either case one has two-electron stabilizing interactions. A substituent will seek out a site and an orientation (if it is "single-faced") that maximizes interaction.[21] If the d orbitals are occupied and the substituent a donor, then one encounters four electron repulsive interactions. The substituent will seek to minimize these. It may also seek interaction with unfilled d levels, but our calculations seem to indicate that these are too high in energy to be significant.

We can thus proceed from the overlaps of Table V to a set of predictions for site preferences of cylindrical $\pi$ substituents and conformational preferences for single-faced donors or acceptors. Table VI summarizes this information, including for completeness the pentagonal-bipyramid case. The calculations that were done with model or specific donors or acceptors are in general accord with these predictions. In some cases, however, the difference in energy between various sites or conformations is not very large. Thus a model CO $ML_6CH_2^+$ prefers a $cf_\perp$ orientation to $cf_\parallel$ by only 1.5 kcal/mol. In other cases the predicted rotational barriers are an order of magnitude larger.

Next we wish to compare these theoretical conclusions with the experimental evidence that is available. This is a hazardous task, for we recognize well that in these inevitably congested molecules the observed geometry may be set in large part or even entirely by the steric requirements of the ligands. Fully aware of this limitation, we nevertheless trace the full implications of the electronic effects analyzed in the previous sections.

In many $d^0$ PB complexes, the donor atoms, typically oxide or halide, preferentially occupy the axial sites. This is true not only for the ubiquitous uranyl systems[30] but also for several Nb(V) and Ta(V) systems.[58]

There is an interesting class of $d^4$ molybdenum and tungsten(II) complexes which have ligand combinations of strong and weak $\pi$ acceptors with donor halides.[5] All known complexes in this class have either CTP or CO structural form. Predicted substituent site preferences (Table VI) in this $d^4$ case give an ordering for the ligand extremes of strong $\pi$ acceptor (carbon monoxide or cyanide) and of strong donors (halide) of

$$\left.\begin{array}{ll} \text{acceptor} & cf > c > uf \\ \text{donor} & uf > c > cf \end{array}\right\} CO$$

$$\left.\begin{array}{ll} \text{acceptor} & qf \sim e > c \\ \text{donor} & c > qf \sim e \end{array}\right\} CTP$$

The stereochemical guide would appear to be in accord with established structures in this class. For example, $Mo(CNR)_6I^+$ is a CTP with the halide at the capping position and $W(CO)_4Br_3^-$ is a CO with carbon monoxide ligands at the capping position and the capped face. Detailed discussion of the other structurally defined members in this class is complicated by the fact that few of these complexes have exact CTP or CO structural form[14c] and some seem to be

intermediate[14] between CTP or CO. In fact, the qualitative descriptions of structural form in the original crystallographic literature occasionally have been incorrect or misleading. Nevertheless, substituent site preferences maintain their validity in applications to alternative forms. The stereochemical features remain qualitatively intact irrespective of the reference (CO or CTP) form because the minor, one-step rearrangement path that interconverts CO and CTP forms (illustrated in Figure 4) permutes the vertex positions in CTP and CO forms in one-to-one correspondence with our substituent site preferences in the two forms as noted below for the unique vertices in the two forms

c in CTP → uf in CO

c in CO → e in CP

This feature is nicely illustrated in the complex $MoBr_2(C-O)_2[(C_6H_5)_2AsCH_2As(C_6H_5)_2]_2$ first described[43] as a CO with the carbon monoxide ligands at the capping position and at one of the capped face vertices, with bromine atoms at uncapped face positions, and with the unique diarsine ligand that is unidentate at a capped face position. An alternative description[14b] is as a CTP with bromines at the capping position and one of the qf positions and carbon monoxide at an e and a qf position. Our substituent site guide is in full accord with the stereochemical description of this complex in either CTP or CO form and the rearrangement mode shown in Figure 4 provides a simple geometrical correlation between the stereochemical descriptions in the two idealized limiting forms. Interestingly, the accurate description of this seven-coordinate complex places it at the midpoint of a path (see Figure 4) connecting the CTP and CO forms.[14c]

Among the $d^0$ complexes in Table II is one CO and four PB. In several of the compounds we are faced with a difficult judgment, one that we would rather not make, between the donor capability of oxide and halide ligands. In the $UO_2(NCS)_5^{3-}$ ion there is a clear partitioning between donors and acceptors, and as expected the former enter the axial sites.

The above discussion has emphasized $ML_7$ structures. There are over 100 crystal structures with one or more bidentate and polydentate ligands.[5] In these the constraint of the chelate ring(s) may become the determinant of both the overall geometry of the complex and the specific location of a substituent atom. Some of the consequences of such chelate constraints have been analyzed by Kepert.[59] In our discussion we mention but a handful of these complexes, those in which a clear distinction between the $\pi$-donating or -accepting characteristics of ligands may be drawn.

There is a series of $d^4$ complexes of the type $M(L-L)(CO)_3X_2$ where the bidentate ligand is a diarsine or a diphosphine, X = Br, Cl, or I, and M = Mo or W. Most are capped octahedra. As expected, the carbonyls are in the capping or capped face sites and the halides in the uncapped face.[60] In $Mo(CO)_4(dppe)(SnCl_3)^+$ the excellent $\pi$ acceptor (and $\sigma$ donor) $SnCl_3$ occupies the capping site of a capped octahedron.[61] $W(CO)_3(bpy)GeBr_3Br$ has a structure intermediate between a CO and a CTP. Viewed as a CTP, it puts the donor Br in the capping site and the acceptors $GeBr_3$ and CO elsewhere.[62] In the more clearly CTP structure of $W(CO)_4(diars)I^+$ the iodide is in the capping site and the carbonyls are located in the unique edge and quadrilateral face,[63] just as we would expect. A similar pattern is found in the CTP $Mo(CO)_2(diars)_2Cl^+$.[64]

In principle the arguments applied to site preferences should also allow us to predict bond strengths. In practice they do not seem to work well. For instance in a $d^4$ CTP system substituted by $\pi$ acceptors the combination of the $\sigma$ effect from **18** and the $\pi$ effect from Tables V and VI would lead one to predict that the bonds to the quadrilateral face ligands should

be strongest. A group of crystal structures by Lippard and co-workers[28,39,47a] of $MoL_6X^+$ and $MoL_7^{2+}$, L = *tert*-butyl isocyanide, definitely show shorter bonds to the two edge ligands.

## Prospects and Limitations

The achievement of this investigation was the development of a molecular orbital view of seven-coordinate complexes wherein a hierarchy of substituent site preferences was established for each of the three major polytopal forms on seven-coordination. These preferences present a stereochemical view in accord with the established structural chemistry in this area. Hence it would appear that our guidelines could be utilized with fair accuracy for the prediction of stereochemistry in the three polytopal forms. Again we note that our predictions do not differ significantly from those that would be based solely on steric arguments—and steric factors are nontrivial considerations in complexes of high coordination number. We did not discern opportunities to differentiate between steric and electronic effects in seven-coordination; the directions of the two effects never seemed to diverge. If our substituent guidelines are to have predictive or rationalization value, it is essential to paint gray, at least with a broad brush, those areas where the guidelines should be applied only with great caution.

This molecular orbital view does not possess the resolution to differentiate among the three dominant polytopal forms in seven-coordination. All three forms are very similar in energy; hence molecular structure on this basis cannot be predicted. This is not a serious flaw—certainly not in a stereochemical sense—because stereochemistry can be fairly accurately assessed in each polytopal form. Most importantly, these preferred stereochemistries in each form are directly correlated by very minor intramolecular rearrangement modes such as the stylized cycle encompassed by the three paths traversing PB, CO, and CTP forms outlined in Figures 3–5. Thus, the guidelines are even applicable to complexes whose polytopal form is intermediate between two of the idealized forms. In this sense the molecular orbital view does have a dynamical range analogous to that developed for five-coordination. Application in this dynamic context would be contraindicated only if there were significant constraints due to chelate ligands and this class of ligands in itself presents complications as discussed below.

Our analysis has been limited to complexes in which the metal atom has $d^0$ through $d^4$ configurations, although there are seven-coordinate complexes based on metal ions of $d^x$ configuration greater than four and also a large set based on lanthanides and actinides.[5,6] The latter set may be characterized as largely electrostatic complexes in which case the $\sigma$-bonding considerations elucidated in the second section of this article may be sufficient for a substituent site preference guide. Actually, the majority of seven-coordinate complexes that lie outside the $d^0$–$d^4$ range are primarily chelate structures.[5,6] Chelate ligands can introduce substantial constraints in structure, stereochemistry, and dynamic stereochemistry. In the extreme case, the molecular structure simply may be a minor extension beyond the preferred structure and conformation of the chelate ligand. A classic example is the seven-coordinate manganese complex based on the sexadentate ethylenediaminetetraacetate ligand and one water molecule.[49] The chelate ligand forms a basket about the manganese and the water molecule sits above this basket on an axis that is nearly a perfect twofold axis. This extreme example should not be structurally viewed in reference to the idealized seven-coordinate forms, nor should it be subjected to stereochemical analysis with the substituent site guide. In these extreme cases, the molecular mechanics approach, as developed

**Table VII.** Extended Hückel Parameters

| Orbital | $H_{ii}$ | Exponents | Orbital | $H_{ii}$ | Exponents |
|---------|----------|-----------|---------|----------|-----------|
| L 1s | −15.0 | 1.300 | Cl 3s | −24.0 | 2.033 |
| C 2s | −21.4 | 1.625 | Cl 3p | −13.0 | 2.033 |
| C 2p | −11.4 | 1.625 | Mo 5s | −9.502 | 1.930 |
| N 2s | −26.0 | 1.950 | Mo 5p | −5.955 | 1.930 |
| N 2p | −13.4 | 1.950 | Mo 4d$^a$ | −12.87 | 4.542 (0.589 86) |
| O 2s | −32.3 | 2.275 | | | 1.901 (0.589 86) |
| O 2p | −14.8 | 2.275 | | | |

$^a$ Two Slater exponents are listed for the 4d functions Each is followed in parentheses by the coefficient in the double-$\zeta$ expansion.

by Kepert,[59] should be used. The middle ground or gray area is difficult to assess. For example, there is a large class of seven-coordinate chelate structures of the form $(chel)_3ML$ or $(chel)_3MX$ with the chelate ligand typically bidentate and uninegative and L a neutral donor and X a charged donor.[5] In lanthanide chemistry, the common form is $(chel)_3ML$ with L most commonly a water molecule. Structural form is described either as CO or CTP with the unique donor ligand typically at the capping site in the CO form and a vertex of the unique edge in CTP form. These stereochemical forms are precisely correlated by the rearrangement mode shown in Figure 4. Stereochemical form in these complexes would seem nicely accommodated by substituent site preferences based on $\sigma$ donors, a feature consistent with a rough characterization of the lanthanide complexes as largely electrostatic. Another common complex set within this chelate class consists of the $d^0$ titanium group $(chel)_3MX$ species.[5,65] Here a common structural form is the pentagonal bipyramid, and in this form the halide donor ligand lies at an axial site, a result that is consistent with $\pi$-donor site preference in the $d^0$ case. The very same structure and stereochemistry is seen in $(trop)_3SnX$ and $(trop)_3SnOH^{66}$ which are $d^{10}$ complexes and in $Mo(dtc)_3L$, L = $NO$,[67] $NS$,[68] $d^4$ cases with an acceptor substituent. Although the preference rules are consistent with molecular structure in this class, structure and stereochemistry may largely result from the dictates of the chelate ligands. These few examples should suffice to illustrate the possible pitfalls in the chelate area.

Molecular structure is sometimes inaccurately described in relation to idealized polytopal forms—even in crystallographic articles. There may be ambiguities in a description if it is referenced to idealized polyhedra. Analytical procedures have been developed for the accurate assessment of shape, and this can be done with precision if all seven ligands are identical. However, if the ligands are not identical, substantial tactical problems arise.[5,14,69] Here, caution should be exercised in the assessment of structure *in relation to idealized polyhedra.*

An important potential application of the substituent site guide is in stereochemically outlining the reaction mechanism in substitution of six-coordinate complexes. The application is simple and will probably prove accurate for the elementary cases wherein a ligand L′ is added to an $ML_6$ complex with all L ligands identical. For this case, possible paths are neatly outlined in the **1 → 2**, **1 → 3**, and **1 → 4** constructions and the resultant stereochemistries, using the new vertex as the L′ site, are those predicted on the basis of $\sigma$-bonding effects. Again these stereochemistries in each of the three polytopal forms are precisely related through minor rearrangements (Figures 3–5). With the introduction of $\pi$-type ligands the reaction path analysis becomes more complicated but remains manageable. If, however, the octahedral complex has non-identical ligands of slightly varying electronic character, a realistic analysis would necessarily be quantitative in character—a requirement that could not be met with our qualitative scheme.

## Appendix

The method of calculation used is the extended Hückel procedure.[70] The metal atom used was Mo, with a double-$\zeta$ 4d function.[71] Coulomb integrals for the metal atom were obtained from a charge iterative calculation on $Mo(CO)_6$, with an assumed quadratic charge dependence of metal $H_{ii}$'s.[72] The various parameters used in the calculations are listed in Table VII. L is a pseudoligand bearing a single 1s orbital.

Bond distances used were M–L = 1.65 Å, M–CO = 1.97 Å, M–CH$_2$ = 2.00 Å, C–O = 1.14 Å, C–H = 1.10 Å, M–N = 2.00 Å, N–H = 1.04 Å, and M–Cl = 2.45 Å.

To probe $\pi$-donor and -acceptor character p orbitals with exponent 1.625 were added to the $\sigma$ ligand L. The p orbital $H_{ii}$ and the total electron count were varied to make the p orbitals strong or weak donors or acceptors as desired.

## References and Notes

(1) There are relatively simple guidelines that to a first approximation provide a perspective for structural inorganic chemistry. Formal systematics are directly applicable to coordination compounds, boron hydrides, and metal clusters. A brief discussion of structural systematics in inorganic chemistry may be found in "Boron Hydrides", E. L. Muetterties, Ed., Academic Press, New York, N.Y., 1975, Chapter 1.
(2) (a) V. W. Day and J. L. Hoard, *J. Am. Chem. Soc.*, **92**, 3626 (1970); (b) see also discussions by J. J. Park, D. M. Collins, and J. L. Hoard, *ibid.*, **92**, 3636 (1970).
(3) J. S. Wood, *Prog. Inorg. Chem.*, **16**, 227 (1972).
(4) E. L. Muetterties and R. A. Schunn, *Q. Rev., Chem. Soc.*, **20**, 245 (1966).
(5) M. Drew, a comprehensive review to be published in *Prog. Inorg. Chem.* (personal communication).
(6) E. L. Muetterties and C. M. Wright, *Q. Rev., Chem. Soc.*, **21**, 109 (1967).
(7) R. J. Gillespie, *Can. J. Chem.*, **38**, 818 (1960).
(8) D. Britton, *Can. J. Chem.*, **41**, 1632 (1963).
(9) T. A. Claxton and G. C. Benson, *Can. J. Chem.*, **44**, 157 (1966).
(10) H. B. Thompson and L. S. Bartell, *Inorg. Chem.*, **7**, 488 (1968). For an excellent discussion of the connections between the VSEPR and MO approaches see L. S. Bartell, *ibid.*, **5**, 1635 (1966); *J. Chem. Educ.*, **45**, 754 (1968); and R. M. Gavin, Jr., *ibid.*, **46**, 413 (1969). For calculations using a Lennard–Jones pair potential see J. B. Kaelberer, R. D. Etters, and J. C. Raich, *Chem. Phys. Lett.*, **41**, 580 (1976).
(11) The general case refers to a coordination complex in which all ligands are unidentate and identical (see ref 12).
(12) E. L. Muetterties, *J. Am. Chem. Soc.*, **91**, 1636 (1969).
(13) (a) D. Britton and J. D. Dunitz, *Acta Crystallogr., Sect. A*, **29**, 362 (1973); (b) R. B. King, *J. Am. Chem. Soc.*, **91**, 7211 (1969).
(14) (a) E. L. Muetterties and L. J. Guggenberger, *J. Am. Chem. Soc.*, **96**, 1748 (1974); (b) J. K. Kouba and S. S. Wreford, *Inorg. Chem.*, **15**, 1463 (1976); (c) S. S. Wreford, personal communication.
(15) N. S. Hush, *Aust. J. Chem.*, **15**, 378 (1962).
(16) (a) S. T. Spees, Jr., J. R. Perumareddi, and A. W. Adamson, *J. Am. Chem. Soc.*, **90**, 6626 (1968); *J. Phys. Chem.*, **72**, 1822 (1968); (b) F. Basolo and R. G. Pearson, "Mechanisms of Inorganic Reactions", 2d ed, Wiley, New York, N.Y., 1967, Chapter 3.
(17) J. L. Hoard and J. V. Silverton, *Inorg. Chem.*, **2**, 235 (1963).
(18) The d-Stix models are especially useful for an examination of polytopal rearrangements: d-Stix, Geodestix, P.O. Box 5179, Spokane, Wash.
(19) (a) W. N. Lipscomb, *Science*, **153**, 373 (1966); (b) E. L. Muetterties, *Rec. Chem. Prog.*, **31**, 51 (1970); (c) E. L. Muetterties, *Acc. Chem. Res.*, **3**, 266 (1970).
(20) (a) An early discussion of the approach of a ligand to an octahedral complex is given by L. E. Orgel, *J. Chem. Soc.*, 4756 (1952); (b) R. L. Oakland and G. H. Duffey, *J. Chem. Phys.*, **46**, 19 (1967); (c) R. M. Gavin, Jr., *J. Chem. Educ.*, **46**, 413 (1969); (d) G. R. Rossman, F.-D. Tsay, and H. B. Gray, *Inorg. Chem.*, **12**, 824 (1973); (e) R. A. Levenson and R. J. G. Dominguez, *ibid.*, **12**, 2342 (1973); R. A. Levenson, *Chem. Phys. Lett.*, **22**, 293 (1973); (f) J. R. Wasson and D. R. Lorenz, *Inorg. Nucl. Chem. Lett.*, **11**, 617 (1975); (g) L. Pauling, *Proc. Natl. Acad. Sci., U.S.A.*, **73**, 1404 (1976).
(21) (a) A. R. Rossi and R. Hoffmann, *Inorg. Chem.*, **14**, 365 (1975); (b) R. Hoffmann, J. M. Howell, and E. L. Muetterties, *J. Am. Chem. Soc.*, **94**, 3047 (1972).

(22) (a) R. E. Rundle, *J. Am. Chem. Soc.*, **85**, 112 (1963); *Rec. Chem. Prog.*, **23**, 195 (1962); *Acta Crystallogr.*, **14**, 585 (1961); (b) R. E. Rundle, *Surv. Prog. Chem.*, **1**, 81 (1963); (c) R. J. Hach and R. E. Rundle, *J. Am. Chem. Soc.*, **73**, 4321 (1951).
(23) W. J. Adams, H. B. Thompson, and L. S. Bartell, *J. Chem. Phys.*, **53**, 4040 (1970); R. E. LaVilla and S. H. Bauer, *ibid.*, **33**, 182 (1960).
(24) H. J. Hurst and J. C. Taylor, *Acta Crystallogr., Sect. B*, **26**, 417, 2136 (1970).
(25) G. M. Brown and L. A. Walker, *Acta Crystallogr.*, **20**, 220 (1966); J. L. Hoard, *J. Am. Chem. Soc.*, **61**, 1252 (1939).
(26) E. J. Jacob and L. S. Bartell, *J. Chem. Phys.*, **53**, 2235 (1970).
(27) R. A. Levenson and R. L. R. Towns, *Inorg. Chem.*, **13**, 105 (1974).
(28) D. L. Lewis and S. J. Lippard, *J. Am. Chem. Soc.*, **97**, 2697 (1975).
(29) Na$_5$ and K$_5$ salts: M. G. B. Drew, P. C. H. Mitchell, and C. Pygall, cited in ref 5. A $C_{2v}$ structure has been suggested for this ion on the basis of infrared and Raman spectra: P. M. Kiernan and W. P. Griffith, *Inorg. Nucl. Chem. Lett.*, **12**, 377 (1976).
(30) (a) A summary of the relevant structural facts may be found in ref 5 and L. Cattalini, U. Croatto, S. Degetto, and E. Tondello, *Inorg. Chim. Acta, Rev.*, **5**, 19 (1971); D. A. Clemente, G. Bandoli, F. Benetollo, M. Vidali, P. A. Vigato, and U. Casellato, *J. Inorg. Nucl. Chem.*, **36**, 1999 (1974). (b) D. W. Hart, T. F. Koetzle, and R. Bau, personal communication.
(31) W. H. Zachariasen, *Acta Crystallogr.*, **7**, 783 (1954).
(32) V. I. Pakhomov, T. A. Kaidalova, and R. L. Davidovich, *Zh. Neorg. Khim.*, **19**, 1823 (1974); *Russ. J. Inorg. Chem. (Engl. Transl.)*, **19**, 993 (1974).
(33) N. K. Dalley, M. H. Mueller, and S. H. Simonsen, *Inorg. Chem.*, **11**, 1840 (1972).
(34) E. G. Arutyunyan and M. A. Porai-Koshits, *Zh. Strukt. Khim.*, **4**, 110 (1963); *J. Struct. Chem. (Engl. Transl.)*, **4**, 96 (1963).
(35) G. Bombieri, E. Forsellini, D. Brown, and B. Whittaker, *J. Chem. Soc., Dalton Trans.*, 735 (1976).
(36) L. Manoilović-Muir, *Inorg. Nucl. Chem. Lett.*, **9**, 59 (1973).
(37) M. G. B. Drew, J. D. Wilkins, and A. P. Wolters, *J. Chem. Soc., Chem. Commun.*, 1278 (1972).
(38) M. G. B. Drew and A. P. Wolters, *J. Chem. Soc., Chem. Commun.*, 457 (1972).
(39) D. F. Lewis and S. J. Lippard, *Inorg. Chem.*, **11**, 621 (1972).
(40) M. G. B. Drew and J. D. Wilkins, *J. Chem. Soc., Dalton Trans.*, 1654 (1974).
(41) A. Mawby and G. E. Pringle, *J. Inorg. Nucl. Chem.*, **34**, 517 (1972).
(42) M. G. B. Drew and J. D. Wilkins, to be submitted for publication; cited in ref 5.
(43) M. G. B. Drew, A. W. Johans, A. P. Wolters, and I. B. Tomkins, *Chem. Commun.*, 819 (1971).
(44) M. Elian and R. Hoffmann, *Inorg. Chem.*, **14**, 1058 (1975).
(45) In (NMe$_4$)[V(OH)(O$_2$)$_3$]·2H$_2$O the OH group caps a triangular face of a trigonal prism formed by the three peroxide groups: R. E. Drew, F. W. B. Einstein, and J. S. Field, to be submitted for publication; cited in ref 5. Reasonable men may differ as to whether the peroxide ligand should be viewed as a bidentate one.
(46) R. Hoffmann, J. M. Howell, and A. R. Rossi, *J. Am. Chem. Soc.*, **98**, 2484 (1976), and references therein.
(47) (a) A similar level scheme has been obtained by S. J. Lippard, private communication. (b) C. T. Lam, P. W. R. Corfield, and S. J. Lippard, to be published.
(48) D. Nicholls, T. A. Ryan, and K. R. Seddon, *J. Chem. Soc., Chem. Commun.*, 635 (1974).
(49) EDTA complexes: S. Richards, B. Pederson, J. V. Silverton, and J. L. Hoard, *Inorg. Chem.*, **3**, 27 (1964); M. D. Lind and J. L. Hoard, *ibid.*, **3**, 34 (1964); M. J. Hamor, T. A. Hamor, and J. L. Hoard, *ibid.*, **3**, 34 (1964); J. J. Stezowski, R. Countryman, and J. L. Hoard, *ibid.*, **12**, 1749 (1973); G. H. Cohen and J. L. Hoard, *J. Am. Chem. Soc.*, **88**, 3228 (1966), and references therein.
(50) 2,6-Diacetylpyridinebis(semicarbazone) complexes: D. Wester and G. J. Palenik, *J. Am. Chem. Soc.*, **95**, 6505 (1973); *ibid.*, **96**, 7565 (1974); U. Rychlewska, R. C. Palenik, R. W. King, and G. J. Palenik, *J. Chem. Soc., Chem. Commun.*, 799 (1975); D. Wester and G. J. Palenik, *Inorg. Chem.*, **15**, 755 (1976).
(51) Dinitratotris(pyridine) complexes: A. F. Cameron, D. W. Taylor, and R. H. Nuttall, *J. Chem. Soc., Dalton Trans.*, 1603, 1608 (1972).
(52) See J. D. Atwood and T. L. Brown, *J. Am. Chem. Soc.*, **97**, 3380 (1975), and footnote 12 in ref 44.
(53) K. Edgar, B. F. G. Johnson, J. Lewis, and S. B. Wild, *J. Chem. Soc. A*, 2851 (1968); R. Kummer and W. A. G. Graham, *Inorg. Chem.*, **7**, 310 (1968); J. W. McDonald and F. Basolo, *ibid.*, **10**, 492 (1971).
(54) R. T. Jernigan and G. R. Dobson, *Inorg. Chem.*, **11**, 81 (1972); M. N. Memering, A. Moradi-Araghi, and G. R. Dobson, *J. Coord. Chem.*, **2**, 271 (1973); M. N. Memering and G. R. Dobson, *Inorg. Chem.*, **12**, 2490 (1973).
(55) I. Ugi, D. Marquarding, H. Klusacek, P. Gillespie, and F. Ramirez, *Acc. Chem. Res.*, **4**, 288 (1971), and references therein.
(56) In an MO calculation on V(CN)$_7$$^{4-}$, Levenson obtained a greater population of the ligand acceptor orbital we would call eq$_\perp$ than of eq$_\parallel$.[20e] This was attributed to the large interligand overlap in the equatorial plane.

(57) The computation was simplified by truncating the orbitals 33–36, which carry small contributions on the ligands, to that part which is on the metal alone. This truncated wave function was renormalized and then transformed to the local coordinate system ($x'$, $y'$, $z'$) appropriate for the calculation of the overlap integrals.

(58) M. G. B. Drew and J. D. Wilkins, *J. Chem. Soc., Dalton Trans.*, 198, 1579 (1974); 2611 (1975); J. D. Wilkins and M. G. B. Drew, *J. Organomet. Chem.*, 69, 111 (1974).

(59) D. L. Kepert, *J. Chem. Soc., Dalton Trans.*, 617 (1974); 963 (1975); *Inorg. Chem.*, 13, 2754, 2758 (1974); J. C. Dewan, K. Henrick, D. L. Kepert, K. R. Trigwell, A. H. White, and S. B. Wild, *J. Chem. Soc., Dalton Trans.*, 546 (1975).

(60) M. G. B. Drew, *J. Chem. Soc., Dalton Trans.*, 1329 (1972); M. G. B. Drew and C. J. Rix, *J. Organomet. Chem.*, 102, 467 (1975); A. Mercer and J. Trotter, *Can. J. Chem.*, 52, 3331 (1974); J. C. Dewan, K. Henrick, D. L. Kepert, K. R. Trigwell, A. H. White, and S. B. Wild, *J. Chem. Soc., Dalton Trans.*, 546 (1975). Some related structures may be found in M. G. B. Drew, *ibid.*, 626 (1972), and A. P. Wolters, Ph.D. Thesis,

University of Reading, 1975, cited in ref 5.

(61) F. W. B. Einstein and J. S. Field, *J. Chem. Soc., Dalton Trans.*, 1628 (1975).

(62) E. M. Cradwick and D. Hall, *J. Organomet. Chem.*, 25, 91 (1970).

(63) M. G. B. Drew and J. D. Wilkins, *J. Organomet. Chem.*, 69, 271 (1974).

(64) M. G. B. Drew and J. D. Wilkins, *J. Chem. Soc., Dalton Trans.*, 2664 (1973).

(65) R. B. Van Dreel, J. J. Stezowski, and R. C. Fay, *J. Am. Chem. Soc.*, 93, 2887 (1971); D. F. Lewis and R. C. Fay, *ibid.*, 96, 3843 (1974).

(66) J. J. Park, D. M. Collins, and L. J. Hoard, *J. Am. Chem. Soc.*, 92, 3636 (1970).

(67) T. F. Brennan and I. Bernal, *Inorg. Chim. Acta*, 7, 283 (1973).

(68) M. Motevalli and M. B. Hursthouse, unpublished work, cited in ref 5.

(69) W. A. Dollase, *Acta Crystallogr., Sect. A*, 30, 513 (1974).

(70) R. Hoffmann, *J. Chem. Phys.*, 39, 1397 (1963); R. Hoffmann and W. N. Lipscomb, *ibid.*, 36, 2179, 3489 (1962); 37, 2872 (1962).

(71) H. Basch and H. B. Gray, *Theor. Chim. Acta*, 3, 458 (1965).

(72) V. I. Baranovskii and A. B. Nikolskii, *Teor. Eksp. Khim.*, 3, 527 (1967).

Contribution from the Department of Chemistry, Wayne State University, Detroit, Michigan 48202, and the Centrul de Chimie, Timisoara, Romania

# Pfeiffer Effect in Tetrahedral and Negatively Charged Octahedral Coordination Compounds

RONALD J. POLLOCK,[1a] STANLEY KIRSCHNER,*[1a] and SEPTIMIA POLICEC[1b]

The Pfeiffer effect can be utilized to study the optical rotatory and related properties of dissymmetric complexes which are difficult or impossible to resolve because of their optical lability. Most Pfeiffer-active systems are based upon optically active (racemic) six-coordinate complex cations. Examples of Pfeiffer-active systems based upon optically active (racemic) four-coordinate, tetrahedral complexes and negatively charged, octahedral complex anions are reported here, in which both optically active organic compounds and complex inorganic compounds are utilized as environment substances.

## Introduction

The Pfeiffer effect is the change in rotation of a solution of an optically active substance (called the "environment" substance) upon the addition of a racemic mixture of dissymmetric, optically labile, complex inorganic compounds.[2] Many Pfeiffer systems have been reported for cationic octahedral complexes in the presence of organic environments.[3,4] The only previously reported case of a tetrahedral complex exhibiting the Pfeiffer effect is for the bis(8-aminoquinoline)zinc(II) ion.[5] Another tetrahedral complex, bis(8-hydroxyquinoline-5-sulfonato)zinc(II) ion $[Zn(QS)_2]^{2-}$, is reported herein to exhibit the Pfeiffer effect with certain environment substances.

The only negatively charged racemic complexes to show a Pfeiffer effect have been complexes with the oxalate dianion as a bidentate ligand.[3,4,6] The complex anion $[Ni(acac)_3]^-$ (acac = acetylacetonato anion) is negatively charged and does not have the oxalate ion as a ligand, and this racemic complex is also reported herein to the exhibit the Pfeiffer effect.

The enantiomers of the $[Co(en)_3]^{3+}$ ion (en = ethylenediamine) have previously been used as Pfeiffer environments for 1,10-phenanthroline (*o*-phen) complexes and, specifically, for the racemic $[Zn(o\text{-phen})_3]^{2+}$ ion.[7] Because of the infrequent use of inorganic complexes as Pfeiffer environments, the $(+)_{589}[Co(en)_3]^{3+}$ enantiomer also is shown herein to be usable as a Pfeiffer environment for the $[Ni(acac)_3]^-$ anion.

## Experimental Section

Optical rotations were determined on a Perkin-Elmer 141 photoelectric polarimeter at a wavelength of 589 nm and a temperature of 23 °C. All optical rotatory dispersion and circular dichroism spectra were determined on a Cary 60 recording spectropolarimeter at 23 °C. The nonpolarized absorption spectra were taken on a Cary 14 recording spectrophotometer at 23 °C.

$(+)_{589}[Co(en)_3]I_3 \cdot H_2O$ was prepared and resolved according to methods reported in the literature.[8,9]

The zinc complex $H_2[Zn(QS)_2]$ (QS = 8-hydroxyquinoline-5-sulfonate) was prepared according to the method of Liu and Bailar.[10] The analyses of the complex did not agree with the empirical formula, so a purification procedure was developed. This procedure was to dissolve 10 g of the complex in 200 ml of water and then filter the undissolved material. The filtrate was then made acidic by adding hydrochloric acid until the pH of the filtrate was approximately 3.5. The analyses of the crystals thus obtained were in accord with the empirical formula.

The synthesis of the $Na[Ni(acac)_3]$ complex was first reported by Dwyer and Sargeson.[11] This complex was obtained from Mr. John Klein and Dr. Richard Lintvedt of Wayne State University and was purified according to a variation of a method described by Klein.[12] The complex (5.0 g) was dissolved in 250 ml of water and vigorously stirred for 1 h. It was then filtered and 750 ml of methanol was added to the filtrate. The solution was left to stand overnight and the $Na[Ni(acac)_3]$ precipitate was filtered and washed with methanol and then with ether. It was dried at room temperature over sulfuric acid. This purification separates the inner complex $[Ni(acac)_2]$ from $Na[Ni(acac)_3]$, and the analysis of the complex agreed with the empirical formula.

All solutions used in the Pfeiffer systems were aqueous, and these systems were prepared by mixing an aliquot of a stock solution of the environment substance with an aliquot of the stock solution of the metal complexes. They were then diluted to the appropriate volume.

Aqueous solutions of *d*-cinchonine hydrochloride and *l*-brucine hydrochloride were prepared from *d*-cinchonine and *l*-brucine by adding hydrochloric acid dropwise until the *d*-cinchonine or *l*-brucine dissolved (ca. 1.5 mol of HCl/mol of alkaloid). The pH of these solutions never went below 3.5.

## Results and Discussion

**The $[Zn(QS)_2]^{2-}$ Systems.** There is a significant difference between the absorption spectrum of the $[Zn(QS)_2]^{2-}$ anion and that of the ligand, $QS^{2-}$ (Figure 1). The doublets of the $QS^{2-}$ anion at 340 and 250 nm converge to singlet peaks at 365 and 255 nm in the spectrum of the complex $[Zn(QS)_2]^{2-}$. The